SOILS AND FOUNDATIONS Vol. 18, No. 2, June 1978
Japanese Society of Soil Mechanics and Foundation Engineering

HYSTERETIC DAMPING OF SANDS UNDER CYCLIC LOADING AND ITS RELATION TO SHEAR MODULUS

FUMIO TATSUOKA*, TOSHIO IWASAKI** and YOSHIKAZU TAKAGI***

ABSTRACT

Comprehensive tests were performed to obtain hysteretic dampings of normally consolidated reconstituted sands with use of a resonant-column apparatus and a static torsional shear device. It is shown that there is a simple relationship between the ratio of shear modulus to the shear modulus at very small strain level and damping ratio for sands tested. This relationship is not affected considerably by void ratio and confining pressure for shear strain amplitude from 10^{-6} to 10^{-2}. For a given value of $G/\{G\}_{\gamma=10^{-6}}$; the ratio of shear modulus to that at $\gamma=10^{-6}$, the values of damping ratio of clean sands tested are slightly larger than those of other reconstituted natural sands. For these two kinds of sand, average curves representing the relationship between damping ratio and $G/\{G\}_{\gamma=10^{-6}}$ are shown. These curves can be used for design purposes to evaluate damping ratio of sands from the value of $G/\{G\}_{\gamma=10^{-6}}$.

Key words: damping, dynamic, sand, special shear test, torsion, vibration
IGC: D6/D7

INTRODUCTION

In performing earthquake response analyses of grounds and soil structures, damping capacities of soils as well as their shear moduli should be evaluated. It is known that decrements of vibration amplitudes in grounds and soil structures are caused mainly by two different phenomena; namely geometric damping and internal damping. Geometric damping can be induced by the fact that vibrations propagate specially in grounds and soil structures. Therefore, geometric damping is inevitable in the case of wave propagations in perfectly elastic media. On the other hand, internal damping is caused by energy dissipation in soil elements. In the course of energy dissipation, some of elastic energy stored in soil elements is consumed for destroying edges and structures of soil grains or transformed into energy of sound, heat etc. In viewing comprehensive studies on the nature of damping in soils, it seems that major parts of internal damping in soils are primarily caused by hysteretic damping which is due to nonlinear characteristics of stress-strain relations of soils, and that the effects of viscous damping is minor (Hardin, 1965; Hara et al., 1973; Sugimoto et al., 1974). As for hysteretic damping of a soil, a damping ratio is fundamentally defined as the ratio of the damping energy or dissipation energy in a soil element per cyclic loading ΔW to the elastic energy or stored energy in the soil element

* Associate Professor, Institute of Industrial Science, Univesity of Tokyo, 22-1, Roppongi 7, Minato-ku, Tokyo, Japan. Formerly, Senior Research Engineer, Public Works Research Institute.
** Chief, Ground Vibration Section, Public Works Research Institute, Ministry of Construction, 4-12-52 Anagawa, Chiba.
*** Assistant Researcher, do.
Written discussions on this paper should be submitted before April 1, 1979.

per cyclic loading W. This definition is well illustrated in Fig. 1. In this paper, notation η defined in Fig. 1 is called damping ratio. Neverthless, other notations D, h or λ_h may be used instead of η.

It is to be noted that damping ratios for hysteretic damping for a specific shear strain amplitude are strain-rate independent, while damping ratios for viscous damping also defined in Fig. 1 are strain-rate dependent. It is known that damping ratios of soils are strain dependent as in the case of shear moduli of soils. By performing a comprehensive test with use of both a resonant-column device and a torsional shear device on hollow cylindrical specimens of various normally consolidated reconstituted sands, Iwasaki, Tatsuoka and Takagi (1978) established a simplified relationship between equivalent shear modulus defined in Fig. 1 and shear strain amplitude as;

$$[G/\{G\}_{\gamma=10^{-6}}]_p = f(\gamma)\cdot p^{m'(\gamma)} \tag{1}$$

In Eq. (1), $[G/\{G\}_{\gamma=10^{-6}}]_p$ means the ratio of the shear modulus at the strain γ of interest larger than 10^{-6} to the shear modulus at $\gamma=10^{-6}$ for the meam principal stress p of interest and $f(\gamma)$ is the value of $[G/\{G\}_{\gamma=10^{-6}}]_p$ for the value of $p=1.0\,\text{kg/cm}^2$. $m'(\gamma)$ is $m(\gamma)-m(\gamma=10^{-6})$, where $m(\gamma)$ is the power of p at γ of interest and $m(\gamma=10^{-6})$ is the value of $m(\gamma)$ at $\gamma=10^{-6}$. The functions $f(\gamma)$ and $m'(\gamma)$ established on the basis of the data of various sands are shown in Fig. 2. Using Eq. (1) and curves shown in Fig. 2, the rate of the decrease in shear modulus with the increase in shear strain amplitude can be easily evaluated.

Herein described are measured hysteretic damping ratios defined in Fig. 1 of various normally consolidated reconstituted sands. Characteristics of shear moduli of these sands have been reported in the previous paper (Iwasaki, Tatsuoka and Takagi, 1978). It has been found that the fashion of the increase in damping ratios of materials including sands are deeply related to the fashion of the decrease in rigidity or shear modulus of these materials (Lazan, 1968; Hardin and Drnevich, 1972 b). In this paper, a simple method for evaluating damping ratios from the value of $G/\{G\}_{\gamma=10^{-6}}$ on the basis of measured shear moduli and damping ratios is shown. This method is based on the theories proposed by Lazan (1968) and Hardin and Drnevich (1972 b). Furthermore, loss moduli of sands tested which represent damping capacities of these sands are discussed.

TEST PROCEDURES

In this study, two devices, namely a resonant-column apparatus and a torsional shear device, were employed. Shear moduli and damping ratios for shear strain amplitude (sin-

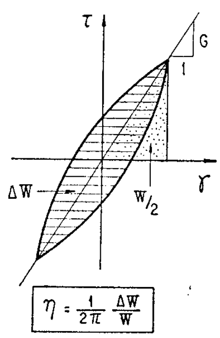

Fig. 1. Definitions of shear modulus and hysteretic damping ratio

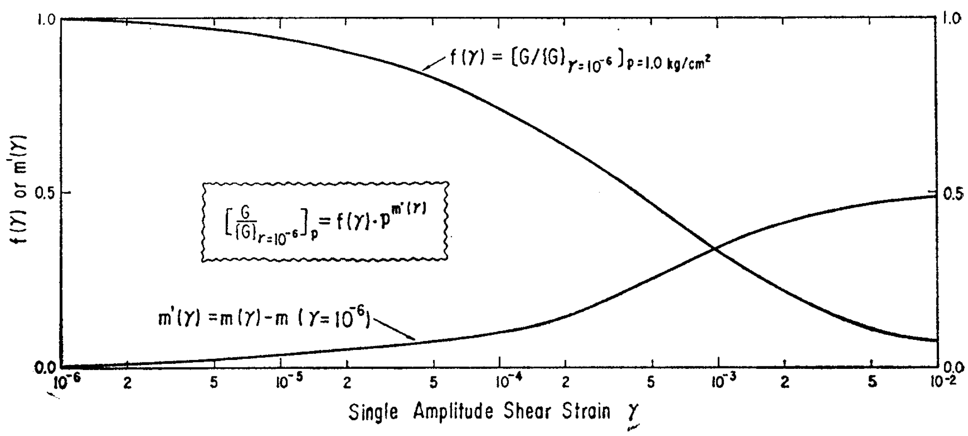

Fig. 2. $f(\gamma)=[G/\{G\}_{\gamma=10^{-6}}]_{p=1.0\text{kg/cm}^2}$ **versus** γ **and** $m'(\gamma)=m(\gamma)-m(\gamma=10^{-6})$ **versus** γ **relationships of sands for design purposes**

Table 1. Test materials and test programs

Material	G_s	D_{10} (mm)	D_{50} (mm)	U_c	e_{max}	e_{min}	F. C.*) (%)	Air-Dry or Saturated	Sample Preparation**)	Density	Confining Pressure p(kg/cm^2)
Toyoura Sand	2.64	0.12	0.162	1.46	0.96	0.64	0.1	A-D	RN	Loose	1.0
								S	SP	Med-Loose	1.0
								A-D, S	SP+TP	Dense, Med-Dense	0.25, 0.5, 1.0, 2.0
Model-Test Sand***)	2.88	0.31	0.48	1.52	0.93	0.66	0.5	Air-Dry	Spooning and Tapping	Dense or Medium-Dense	1.0
Ban-nosu Sand A	2.67	0.168	0.26	1.70	1.17	0.82	1.1				
〃 B	2.66	0.31	0.92	3.35	1.01	0.68	0.5				
〃 C	2.68	0.15	0.34	2.73	1.03	0.69	5.9				
〃 15	2.67	0.24	0.88	4.58	0.91	0.69	0.26				
〃 18	2.67	0.31	0.99	1.20	0.94	0.68	0.5				
〃 21	2.67	0.25	0.72	3.60	0.92	0.67	0.8				
Iruma Sand	2.75	0.28	0.50	1.98	0.84	0.57	0.6				
Ohgi-Shima Sand	2.69	0.20	0.37	2.25	0.72	0.49	0.36				1.0, 2.0
Kinjo Sand 1	2.66	0.16	0.42	2.88	1.11	0.71	3.0				1.0
Kinjo Sand 2	2.67	0.09	0.32	3.89	1.42	0.92	8.8				
Monterey No. 0 Sand	2.65	0.32	0.44	1.38	0.85	0.56	0.0				

*) F. C. ; Content of Finer Soils than 0.074 mm.
**) SP ; Spooning Method, SP+TP ; Spooning and Tapping Method, RN ; Raining Method.
***) After oven-dried several times.

gle amplitude) γ ranging from 10^{-6} to 10^{-4} were obtained from resonant-column testings and those for γ ranging from 10^{-4} to 10^{-2} were obtained from torsional shear testings. In both tests, hollow cylindrical specimens were used. The height of the specimen is 25 cm in resonant-column testings and 10 cm in torsional shear testings. The inner and outer diameters are 10 cm and 6 cm, respectively, for both testings. Measurements of shear moduli and damping ratios in both testings were performed on specimens which are isotropically and normally consolidated under various confining pressures. Physical properties and test conditions for various sands are listed in Table 1. For pouring sand, two methods, namely spooning method and raining method, were employed. In the spooning method, air-dry sands were poured with a spoon into a mold, and de-aired saturated sands were also poured with a spoon into a mold which had been filled with de-aired water in advance. Densification was performed by tapping the mold with a small wooden hammer. In the raining method, air-dry sands were poured from a constant height of 10 cm above sand surfaces into a mold through a small hole with the diameter of 3 mm. In torsional shear tests, samples were sheared cyclicly by ten times first at shear strain amplitude of about 7×10^{-5} by controlling shear stress amplitude. The samples were repeatedly sheared cyclicly at increased shear strain levels until a shearing failure occurrs. The frequency of cyclic loading was 0.1 Hz. Damping ratios at the tenth cyclic loading are taken as the representative values in the present study. Variation of damping ratio with respect to the number of cyclic loadings will also be discussed. All the tests were performed under fully drained conditions. Those devices, test procedures, and properties of sands tested are described in detail in the previous papers (Kuribayashi, Iwasaki and Tatsuoka, 1975; Iwasaki and Tatsuoka, 1977; Iwasaki, Tatsuoka and Takagi, 1978).

FACTORS AFFECTING DAMPING RATIO

Hardin and Drnevich (1972 a) have indicated four parameters; namely strain amplitude γ, effective mean principal stress p, void ratio e and number of cycles of loading N, as important factors affecting damping ratios of sands. To establish a relationship between damping ratios and shear moduli in which the factors affecting damping ratios are incorporated, it is firstly necessary to examine the effects of each of the parameters on damping ratios.

Effects of Shear Strain Amplitude

Figs. 3 and 4 show damping ratios of Toyoura Sand and Ban-nosu Sands for $p=1.0\,\mathrm{kg/cm^2}$ which were obtained by both of resonant-column tests and torsional shear tests. White symbols in Figs. 3 and 4 represent damping ratios measured by means of resonant-column tests and defined as

$$\eta=\frac{1}{2\pi}\Delta_t \qquad (2)$$

where Δ_t is the logarithmic decrement during the first five cycles of free vibration which is recorded after turning off the input power at the resonant state. Damping ratios obtained from Eq. (2) were plotted against the single amplitude shear strains at the stationary resonant state γ_s. Shear strain amplitudes decrease during free vibrations. The shear strain amplitude at the third cycle from the beginning of the free vibrations is expressed by the values of γ_s and η as

$$\gamma_3=\exp(-3\cdot\Delta_t)\cdot\gamma_s=\exp(-6\pi\cdot\eta)\gamma_s \qquad (3)$$

If the relationship between η and γ_s is known, the relationship between η and γ_3 can be derived with use of Eq. (3). The relationships between η and γ_3 are shown by a broken curve in Fig. 3. The differences between the values of η for the same values of

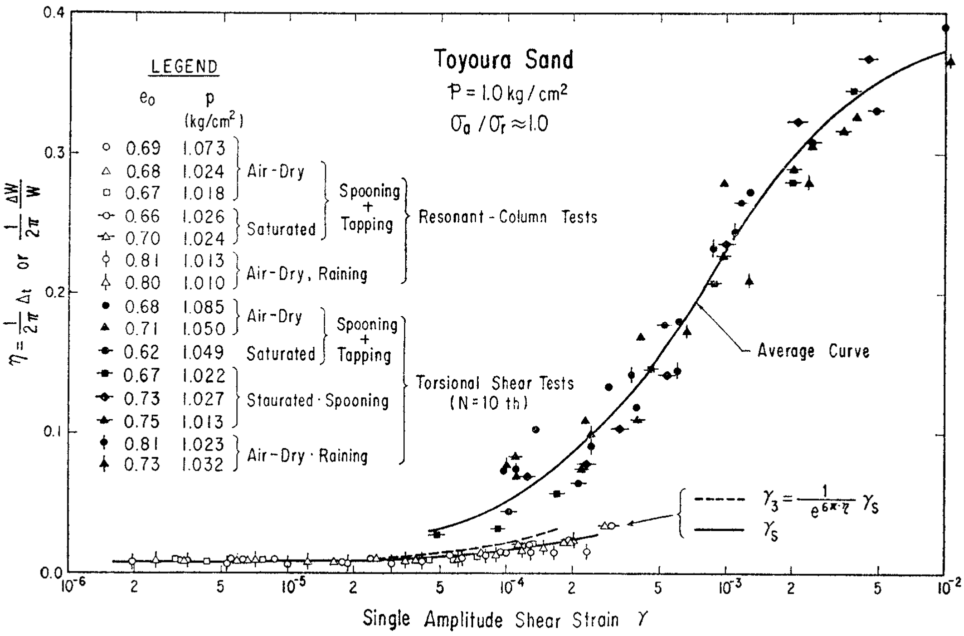

Fig. 3. η versus γ relationship for $p=1.0\,\mathrm{kg/cm^2}$ of Toyoura Sand

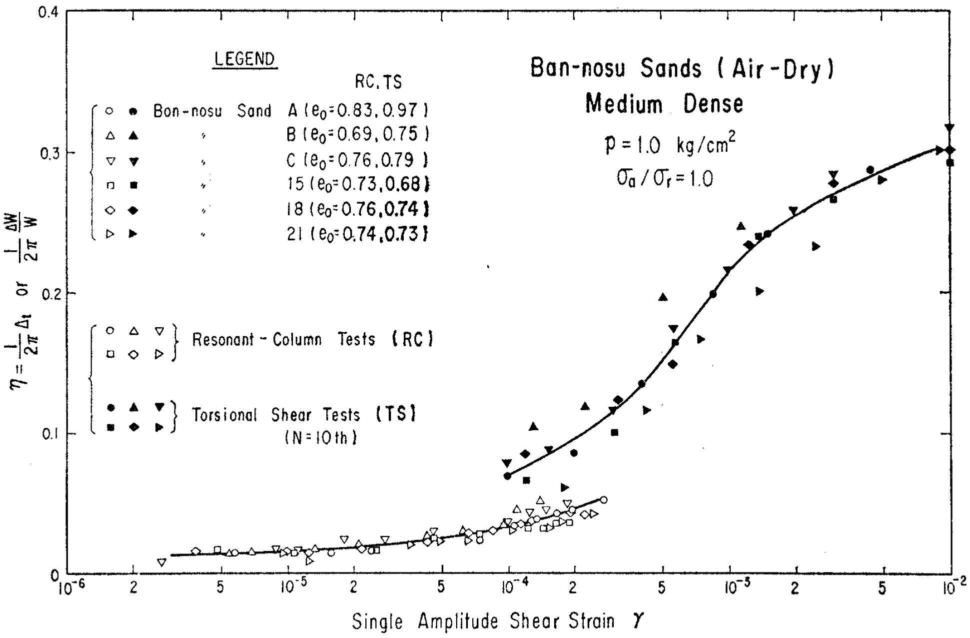

Fig. 4. η **versus** γ **relationship for** $p=1.0\,\mathrm{kg/cm^2}$ **of Ban-nosu Sands**

γ_s and γ_3 is not large for the shear strain amplitude less than 10^{-4}. Therefore, while γ_3 represents the average shear strain amplitude during the first five cycles of the free vibration more adequately than γ_s, γ_s is used for representing the shear strain amplitude during the free vibration in this study. Damping ratios by torsional shear tests shown in Figs. 3 and 4 are those at the tenth cyclic loading.

It is seen from these figures that damping ratios increase with the increase in shear strain amplitude, especially for the range of the shear strain amplitudes larger than 10^{-4} as having been indicated in the previous studies (Silver and Seed, 1971; Hardin and Drnevich, 1972 a). This tendency will be compared, in the later of this paper, with the fact that shear moduli decrease with the increase in shear strain amplitudes.

Effects of Void Ratio

It is seen from Fig. 3 that there is no clear effects of void ratio on damping ratios obtained by the two testing methods. This is more clearly illustrated in Fig. 5 where the damping ratios for $p=1.0\,\mathrm{kg/cm^2}$ of Toyoura Sand are shown. In this figure, TS and RC represent torsional shear tests and resonant-column tests, respectively. The fact that void ratio does not have significant effects on damping ratios of sands which is shown in Fig. 5 is well consistent with that obtained from simple shear tests on clean air-dry sand by Silver and Seed (1971). Considering also that Hardin and Drnevich (1972 a) did not show any experimental evidence of the effects of void ratio on damping ratio for clean sands, it may be concluded that the effects of void ratio or density on damping ratios of sands can be negligible.

Effects of Number of Cyclic Loading

It is noted from Figs. 3 and 4 that there are some differences between damping ratios obtained by resonant-column tests and those obtained by torsional shear tests even at the same shear strain amplitude of 10^{-4}. In the authors' best knowledge, it is likely that these differences are caused mainly by the effects of the number of cyclic loading. In resonant-column tests in this study, damping ratios at any shear strain amplitude were measured after several thousand cyclic loadings. On the other hand, damping ratios in tor-

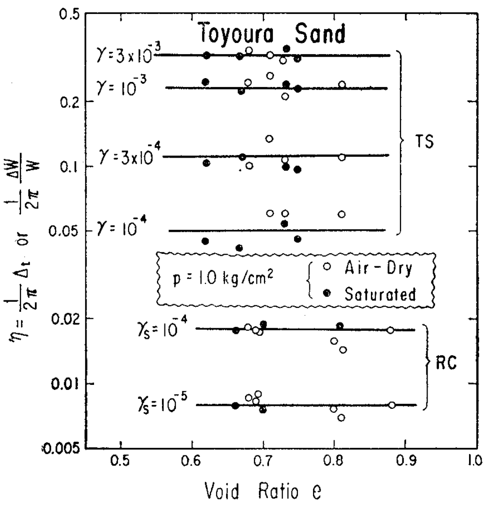

Note; TS means torsional shear tests and RC means resonant-column tests

Fig. 5. η **versus void ratio relationship for** $p=1.0\,\mathrm{kg/cm^2}$ **of Toyoura Sand**

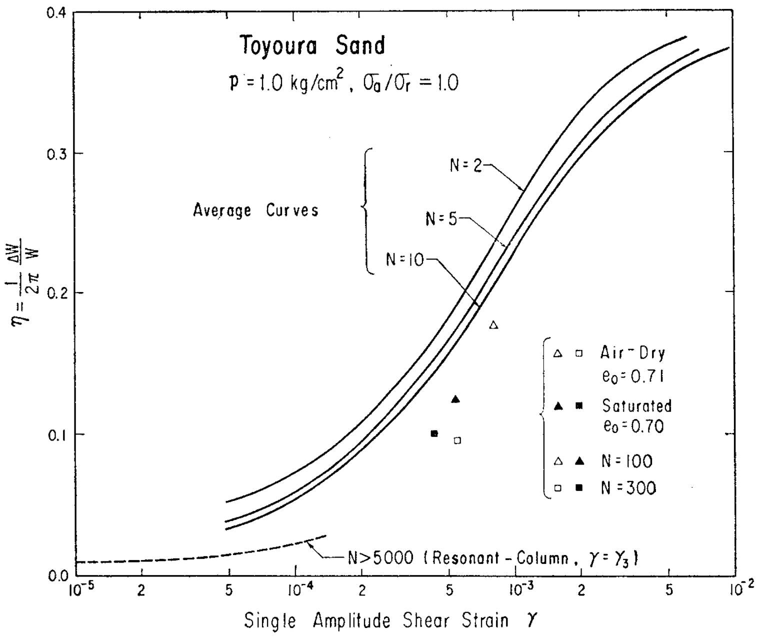

Fig. 6. **Effects of repeated loading on** η **versus** γ **relationship for** $p=1.0\,\mathrm{kg/cm^2}$ **of Toyoura Sand**

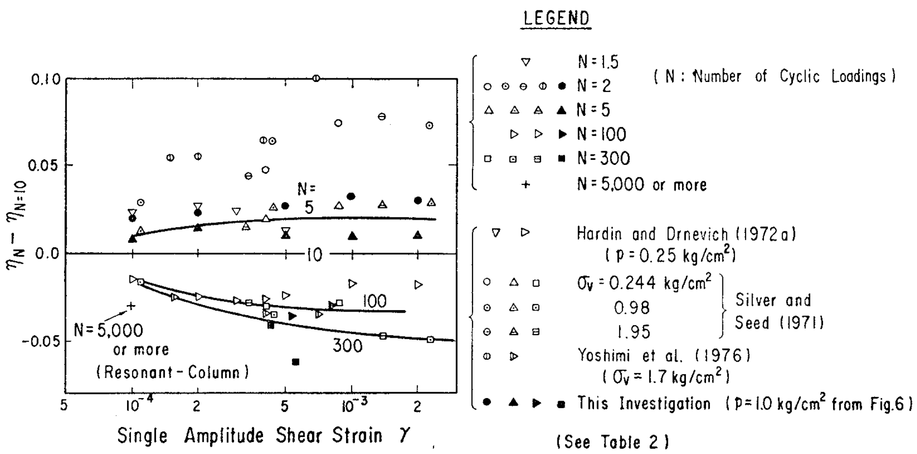

Fig. 7. $\eta_N-\eta_{N=10}$ **versus** γ **relationship of several sands**

sional shear tests which are shown in Figs. 3 and 4 were determined at the tenth cyclic loading at any shear strain amplitude. To illustrate the effects of the number of cyclic loading on damping ratios, shown in Fig. 6 are the average curves of damping ratios in torsional shear tests on Toyoura Sand for the second, the fifth and the tenth cyclic loadings in the case of $p=1.0\,\mathrm{kg/cm^2}$. These curves were obtained by the procedures shown in Fig. 3. Also shown in this figure are damping ratios by resonant-column tests which are plotted against γ_3. It may be seen from Fig. 6 that there are considerable variations in damping ratios with the number of cyclic loading even around the shear strain amplitude of 10^{-4}. To obtain damping ratios at a large number of cyclic loadings more than 10, two additional tests were porformed. In these tests, each sample was subjected to cyclic shear loadings up to 300 cycles by controlling shear stress amplitude. The results of these tests are also plotted in Fig. 6. From these data and the results by other investigations, the differences between the damping ratio at the Nth cyclic loading and that at the 10th cyclic loading were calculated and plotted in Fig. 7 as functions of shear strain amplitude. Although a large scattering is in Fig. 7, it is indicated that the general trend of the data by this investigation including those by resonant-column tests are compatible with the other data. Therefore, it is likely that a large part of the difference at the shear strain amplitude of around 10^{-4} between damping ratio at the 10 th cyclic loading in torsional shear tests and that at the several thousandth cyclic loading in resonant-column tests is mainly due to the difference in the number of cyclic loading. Therefore, the data by torsional shear tests will be mainly used in this paper, because the data at around the 10 th cyclic loading are useful for actual earthquake response analyses. Additional studies are necessary in this respect.

Effects of Confining Pressure

Average curves of damping ratios for each confining pressure obtained by resonant-column tests and torsional shear tests are illustrated in Fig. 8. As seen in Fig. 8, damping ratios decrease with increasing confining pressure, as indicated previously (Silver and Seed, 1971; Hardin and Drnevich, 1972 a). To quantitatively examine the fashion of variation of damping ratios of Toyoura Sand with the change in confining pressure, damping ratios were plotted against confining pressure on full-logarithmic graphs in Figs. 9 and 10. It is seen from these figures that the damping ratios by resonant-column tests and torsional shear tests decrease linearly on the full-logarithmic scale with increasing confining pressure. Then, the damping ratio of Toyoura Sand is represented by the following equation for the range from $p=0.25$ to $2.0\ \mathrm{kg/cm^2}$.

$$\eta=\eta_0(\gamma)\,(p/p_0)^{n(\gamma)} \tag{4}$$

in which $\eta_0(\gamma)$ is the damping ratio at the confining pressure $p=p_0$ and is a function of shear strain amplitude, p_0 is a confining pressure ranging from 0.25 to $2.0\ \mathrm{kg/cm^2}$ and $n(\gamma)$, which is a function of shear strain amplitude, represents the power of confining pressure which has a negative value. The values of $n(\gamma)$ obtained from Figs. 9 and 10 are shown in Fig. 11 in which the data by other investigators are also shown. Hardin (1965) proposed an empirical equation for damping ratio of clean dry sands for shear strain amplitude of 10^{-4} or less and for confining pressure of $p=0.24$ to $1.63\ \mathrm{kg/cm^2}$ on the basis of

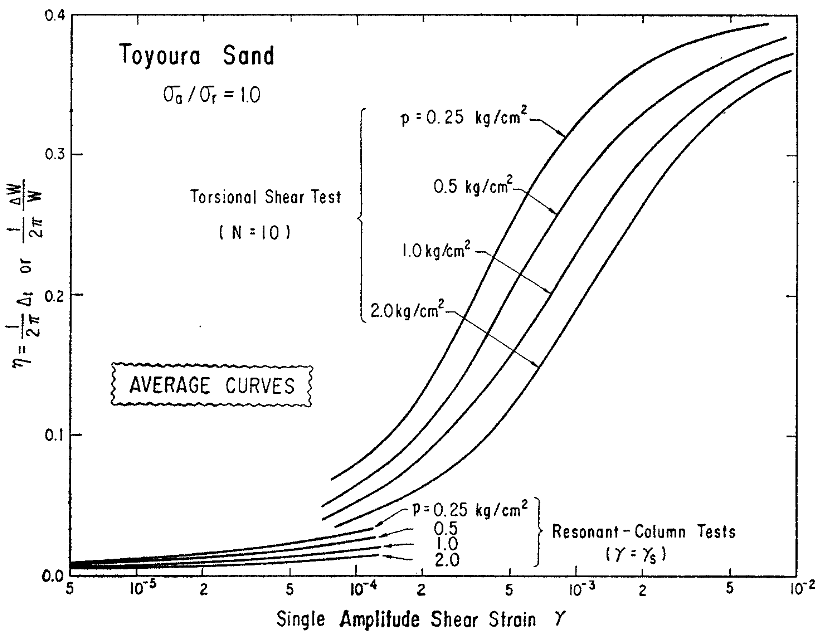

Fig. 8. Average curves of η versus γ relationship for several confining pressures of Toyoura Sand

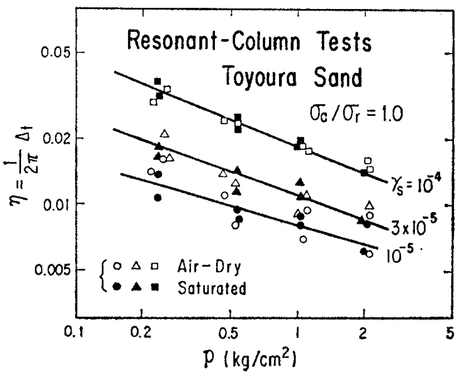

Fig. 9. η versus p relationship by resonant-column tests on Toyoura Sand

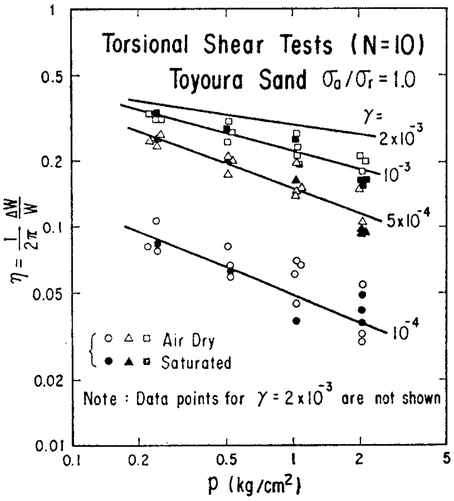

Fig. 10. η versus p relationship by torsional shear tests on Toyoura Sand

comprehensive resonant-column tests, as

$$\eta=\frac{1}{10}\gamma^{0.2}p^{-0.5} \tag{5}$$

The value of $n(\gamma)$ indicated in Eq. (5) is -0.5. This is drawn in Fig. 11. Although available data are quite limited at present and considerable scatterings in the data may be seen in Fig. 11, it is noted that the value of $n(\gamma)$ decreases slightly with increasing shear strain amplitude up to $\gamma=10^{-4}$ and then increases considerably with increasing shear strain amplitude from $\gamma=10^{-4}$ to 10^{-2}. In general, it is rather laborious and expensive to experimentally evaluate damping ratios of sands for a wide range of confining pressure. When the value of damping ratio η_0 of a sand of interest at a specific confining pressure p_0 is available, the approximate values of damping ratios at other confining pressures ranging from 0.25 to 2.0 kg/cm² can be estimated from Eq. (4) using the measured values of η_0 and the values of $n(\gamma)$ obtained in this investigation which is illustrated in Fig. 11.

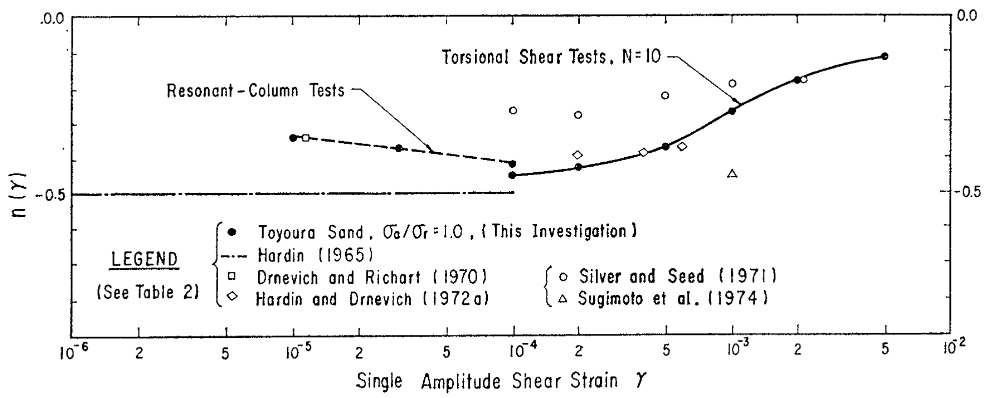

Fig. 11. $n(\gamma)$ versus γ relationships of several sands

Table 2. List of other investigations

Symbol in Fig. 11	Sand	Device	Sample	N *) in Fig. 11	σ_a/σ_r**)	σ_v or p (kg/cm²)	References
—·—·—	Clean Dry Sands	Resonant-Column (RC)	Solid Cylinder	—	1.0	p=0.24～1.63	Hardin (1975)
□	Dry Ottawa Sand No. 30-50	RC (Drnevich)	Hollow Cylinder	—	1.0	p=0.22～0.98	Drnevich and Richart (1970)
◇	Clean Dry Sand	Torsional Shear	〃	100 th	1.0	p=0.248～0.895	Hardin and Drnevich (1972, a)
	Dry Toyoura Sand	Ring Torsion	Hollow Cylinder	—	PS	σ_v=1.70	Yoshimi et al. (1976)
○	Dry Silica Sand No. 20	NGI-Simple Shear	Circular	5 th	PS	σ_v=0.24～1.95	Silver and Seed (1971)
△	—	Simple Shear	Box	—	PS	σ_v=0.205～0.955	Sugimoto et al. (1974)

Note : *) N ; Number of Cyclic Loadings (— ; unknown)
**) PS ; Plane Strain Condition

Effects of Nature of Sand

It may be seen from Figs. 3 and 4 that the damping ratio of Toyoura Sand is slightly larger than those of Ban-nosu Sands especially in larger shear strain amplitudes. Actually, the damping ratios of clean sands, Toyoura Sand and Monterey No. 0 Sand are slightly larger than those of the other sands tested in this investigation. But the variation of damping ratio among the sands other than those two clean sands is small. This will be again discussed later in this paper.

Effects of Methods of Sample Preparation

In this investigation, the samples of Toyoura Sand were prepared by three different methods. However, it can be seen from Fig. 3 that the methods of sample preparation adopted in this investigation have little effects on damping ratios of Toyoura Sand for both resonant-column tests and torsional shear tests. The methods adopted in this investigation are rather limited. Therefore, additional investigations are necessitated to clarify the effects of other methods of sample preparation.

RELATIONS BETWEEN SHEAR MODULUS AND DAMPING RATIO

Lazan (1968) has shown theoretically that the fashion of variation of the damping ratios of elasto-plastic materials can be related to that of the shear moduli of the materials. Similarly to Lazan (1968), Hardin and Drnevich (1972 b) proposed a simple but useful relation between damping ratios and shear moduli of soils. The framework of their theory is illustrated in Fig. 12. This theory is based on the following two postulates:

(i) the ratio of the area $\varDelta W$ shown in Fig. 12 which represents damping energy dissipated in a unit mass per cycle to the area $\varDelta_{abc}$ shown in Fig. 12 is constant irrespectively of the value of shear modulus and,

(ii) damping ratio has its maximum value when shear modulus becomes zero.

By the postulate (i) and using notations shown in Fig. 12, the following equation is derived.

$$\left.\begin{aligned} \varDelta W &= 2K_1\varDelta_{abc} = 2K_1(2\gamma_{apl}\cdot\tau_a) \\ &= 4K_1(\gamma_a-\gamma_e)\tau_a \\ &= 4K_1\left(\frac{1}{G}-\frac{1}{G_{\max}}\right)\tau_a{}^2 \\ W &= \tau_a\cdot\gamma_a = \tau_a{}^2/G \end{aligned}\right\} \qquad (6)$$

Then, by the definition of Eq. (1),

$$\eta=\frac{\varDelta W}{2\pi W}=\frac{2K_1}{\pi}\left(1-\frac{G}{G_{\max}}\right) \qquad (7)$$

where K_1 is a constant. Then, by the postulate (ii), η becomes its maximum value $\eta_{\max}$ when $G=0$ as

$$\eta_{\max}=\frac{2K_1}{\pi} \qquad (8)$$

By combining Eqs. (7) and (8),

$$\eta=\eta_{\max}\left(1-\frac{G}{G_{\max}}\right) \qquad (9)$$

In Eq. (9), $G_{\max}$ means the maximum value of G which is attained when only an elastic shear strain γ_e occures. It is to be noted that if the two postulates are reasonable, Eq. (9) holds irrespectively of the values of void ratio e, confining pressure p and shear strain amplitude γ. To examine the validity of Eq. (3) for sands tested in this investigation, the relationships between η and $G/\{G\}_{\gamma=10^{-6}}$,

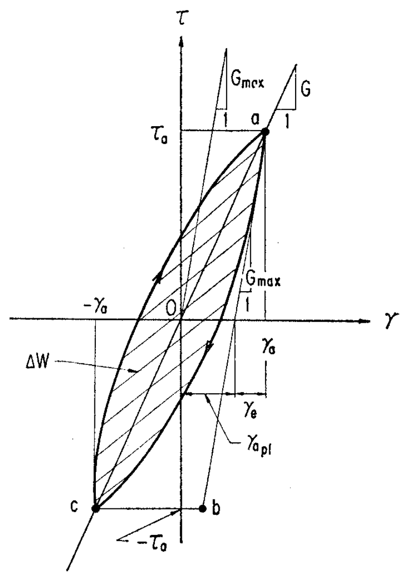

Fig. 12. Stress-strain hysteresis loop for reversed loading

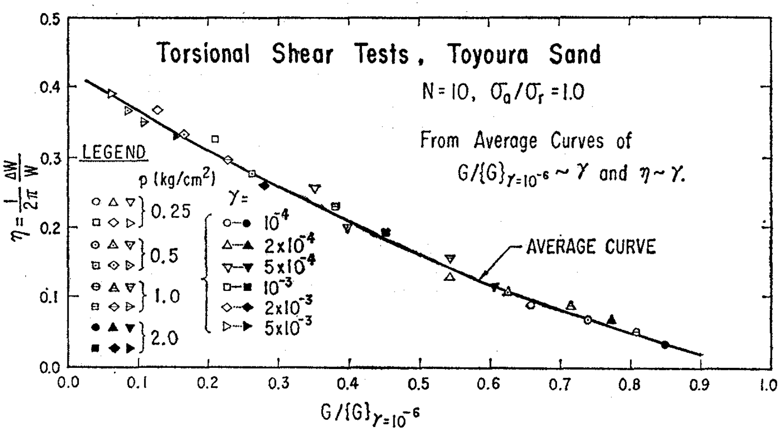

Fig. 13. η versus $G/\{G\}_{\gamma=10^{-6}}$ relationship of Toyoura Sand (N=10)

in place of G/G_{max}, were obtained as follows. For Toyoura Sand, it has been shown that $G/\{G\}_{\gamma=10^{-6}} \sim \gamma$ relationships are not affected considerably by void ratio. The average relationships of $G/\{G\}_{\gamma=10^{-6}}$ versus γ for p=0.25, 0.5, 1.0 and 2.0 kg/cm² for Toyoura Sand were established and shown in Fig. 14 in the previous paper (Iwasaki, Tatsuoka and Takagi, 1978). Also it is shown in Fig. 5 that damping ratios are not affected by void ratio for Toyoura Sand and the average curves of η versus γ for p=0.25, 0.5. 1.0 and 2.0 kg/cm² are illustrated in Fig. 8. The two average curves, $G/\{G\}_{\gamma=10^{-6}}$ versus γ and η versus γ, were established on the base of test results. From these average curves, the values of η and $G/\{G\}_{\gamma=10^{-6}}$ at $\gamma=10^{-4}$, 2×10^{-4}, 5×10^{-4}, 10^{-3}, 2×10^{-3} and 5×10^{-3} for each confining pressure were read off and plotted in Fig. 13. It is seen clearly in Fig. 13 that there is an almost linear relationship between η and $G/\{G\}_{\gamma=10^{-6}}$ and that this relationship is uniquely determined irrespectively of p. The average curve of $\eta \sim G/\{G\}_{\gamma=10^{-6}}$ relationship shown in Fig. 13 was established for the number of cyclic loading N of 10 and damping ratios by resonant-column tests were not utilized to make this line. To examin the effects of the number of cyclic loading on $\eta \sim G/\{G\}_{\gamma=10^{-6}}$ relationship, the values of η and $G/\{G\}_{\gamma=10^{-6}}$ for N=2 and 5 in the case of p=1.0 kg/cm² were read off from Fig. 6 in this paper and Fig. 15 in the previous paper (Iwasaki, Tatsuoka and Takagi, 1978) and plotted in Fig. 14. It can be seen in Fig. 14 that the data points for N=5 locate almost on the average curve for N=10 but the points for N=2 locate slightly above the average curve. Although it is also anticipated that the relationship between η and $G/\{G\}_{\gamma=10^{-6}}$ for the larger number of N than 10 will locate slightly below the average curve for N=10,

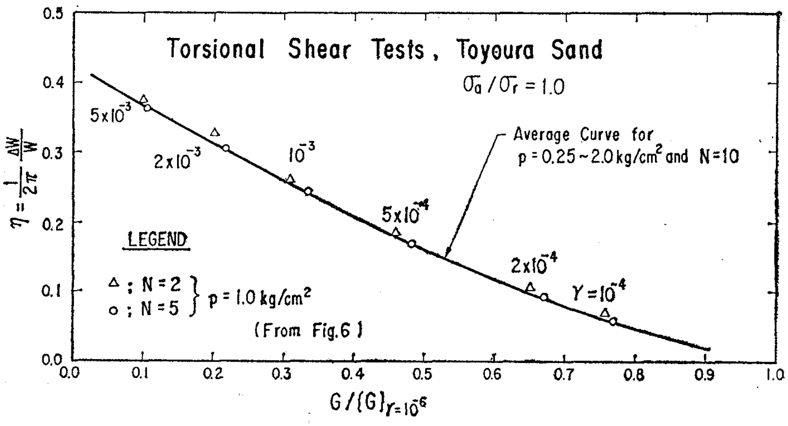

Fig. 14. η versus $G/\{G\}_{\gamma=10^{-6}}$ relationship of Toyoura Sand (N=2, 5 and 10)

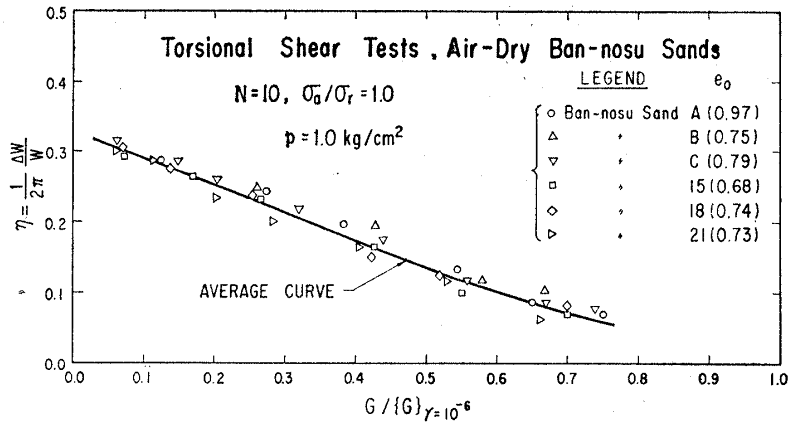

Fig. 15. η **versus** $G/\{G\}_{\gamma=10^{-6}}$ **relationship of Ban-nosu Sands** ($p=1.0\,\mathrm{kg/cm^2}$)

it can be said that for N ranging from 2 to 10, the relationship between η and $G/\{G\}_{\gamma=10^{-6}}$ is not affected strongly by the number of cyclic loading.

Combined with the fact that $G/\{G\}_{\gamma=10^{-6}}\sim\gamma$ relationships and $\eta\sim\gamma$ relationships, from which Fig. 13 was made, are not affected by void ratio, it may be concluded that the relationship between η and $G/\{G\}_{\gamma=10^{-6}}$ of Toyoura Sand can be determined uniquely irrespectively of the values of void ratio, confining pressure, shear strain and number of cyclic loading within their ranges adopted in this investigation. This is the same characteristics as indicated by Eq. (9). Neverthless, it may be seen by carefully examining the relationship shown in Figs. 13 and 14 that this relationship should be represented by a slightly curved line instead of a straight line. In Figs. 15 and 16 shown are the relationships of η versus $G/\{G\}_{\gamma=10^{-6}}$ of the other sands tested in this investigation and the relationship of η versus $G/G_{\max}$ of a clean dry sand tested by Hardin and Drnevich (1972 b). From Figs. 13, 14 and 15, it is seen that all the data of η versus $G/\{G\}_{\gamma=10^{-6}}$ or $G/G_{\max}$ available at present are well expressed by slightly curved lines rather than straight lines. Therefore, the relationship of η versus $G/\{G\}_{\gamma=10^{-6}}$ can be represented in a more general form than Eq. (9) as

$$\eta=\eta_{\max}\,g(X) \tag{10}$$

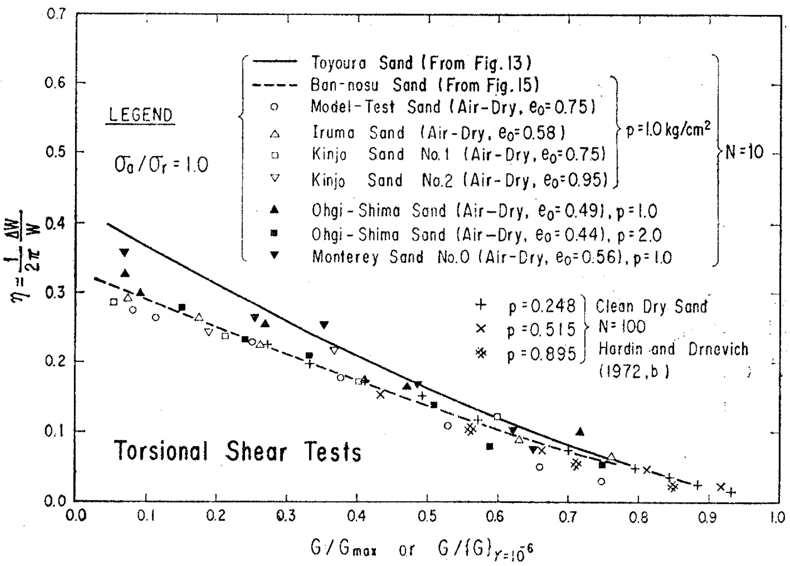

Fig. 16. η **versus** $G/G_{\max}$ **or** $G/\{G\}_{\gamma=10^{-6}}$ **relationship of sands**

in which η_{max} is the maximum damping ratio for $G=0$ and varies with the kind of sand, X is defined as $G/\{G\}_{\gamma=10^{-6}}$, and $g(X)$ is a function of X. The function $g(X)$ may be determined uniquely irrespectively of the kind of sands. It can be easily anticipated from the data shown in Figs. 13, 15 and 16 that if these data are plotted on $\eta/\eta_{max}\sim G/\{G\}_{\gamma=10^{-6}}$ or G/G_{max} graphs, all the data will locate within a very narrow band. This is because the trends of variations of η with the variations of $G/\{G\}_{\gamma=10^{-6}}$ or G/G_{max} are very similar for all the data. Therefore, it is reasonable to define the function $g(X)$ independently of the kind of sand. Also it is seen from Figs. 13, 15 and 16 that the value of η_{max} which is attained when $G=0$ varies with the kind of sand. The test results obtained by this investigation which are illustrated in Fig. 16 show that the values of η_{max} of Toyoura Sand and Monterey Sand No. 0, both being clear sands, are slightly larger than those of the other natural sands which are non-clean sands including fine particles less 0.074 mm to some extent.

The $\eta\sim G/\{G\}_{\gamma=10^{-6}}$ relationship obtained in this investigation were compared with those obtained by other investigations in Fig. 17. In this figure, the average curve for Toyoura Sand which can also be used for that of Monterey Sand No. 0 and the average curve for the other natural sands are shown. Also shown in this figure are (i) the line derived from the $G/\{G\}_{\gamma=10^{-6}}\sim\gamma$ relationship and the $\eta\sim\gamma$ relationship for sands proposed by Seed and Idriss (1970), (ii) the lines by Eq. (9) using the values of η_{max} which can be obtained by substituting $N=10$ into the following equations which were proposed by Hardin and Drnevich (1972 b),

$$\eta_{max}=\{33-1.5(\log_{10}N)\}/100 \quad \text{for clean dry sand} \tag{11}$$

$$\eta_{max}=\{28-1.5(\log_{10}N)\}/100 \quad \text{for clean saturated sand} \tag{12}$$

and (iii) the line which was derived from the empirical equations in respect of shear modulus and damping ratio of dry Ottawa Sand by Sherif and Ishibashi (1976) and Sherif, Ishibashi and Gaddah (1977). Their empirical equations for strain-dependancy of shear modulus were quoted and compared with others in the previous paper (Iwasaki, Tatsuoka and Takagi, 1978). Sherif, Ishibashi and Gaddah (1977) established an empirical equation for damping ratio of dry Ottawa Sand at the second cyclic loading in torsional shear tests as

$$\eta=33.95(5.86-p)\gamma^{0.3} \tag{13}$$

in which η and γ are decimals and p is in kg/cm². The line shown by the dotted line in Fig. 17 is the one for $p=1.0$ kg/cm² which was derived from the equation for strain-dependency of shear modulus and Eq. (13). It is seen in Fig. 17 that the differences

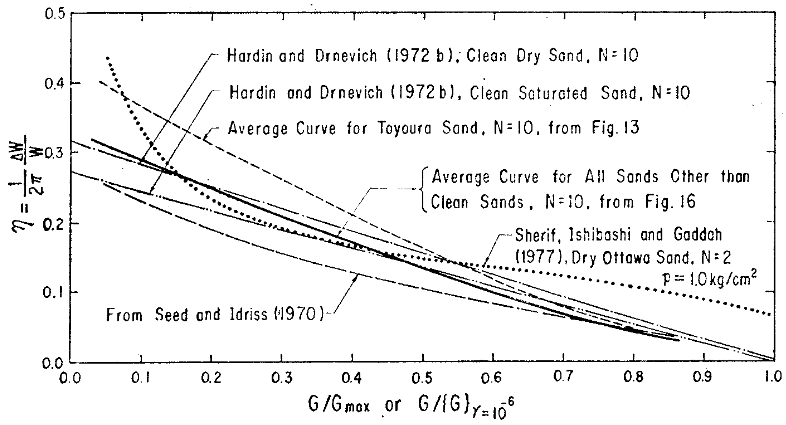

Fig. 17. Comparison among η versus G/G_{max} or $G/\{G\}_{\gamma=10^{-6}}$ relationships

among shapes of lines is rather small except the line by Sherif, Ishibashi and Gaddah (1977). It is likely that the value of η becomes unusual ones when $G/G_{\max}$ becomes 1.0 or 0.0 in the case of $\eta \sim G/G_{\max}$ relationship by Sherif, Ishibashi and Gaddah (1978). Among the other five lines, the average curve for Toyoura Sand locates in the slightly upper part and the line by Seed the Idriss (1970) situates in the lower part. And the average curve of the all natural sands other than the two clean sands may be found to be the average curve for the five curves other than the one by Sherif, Ishibashi and Gaddah (1977). From these facts, it would be reasonable to utilize the average curve of the natural sands other than the two clean sands, which is drawn by a solid curve in Fig. 17, to evaluate approximate values of η of ordinary natural sands. The value of $G/\{G\}_{\gamma=10^{-6}}$, which is needed to evaluate the value of η using the solid curve shown in Fig. 17, can be estimated from Eq. (1) using two curves illustrated in Fig. 2.

LOSS MODULUS OF TOYOURA SAND

Non-linear stress-strain relationships of sands can be generally expressed by equivalent linear stress-strain relationships as

$$\bar{\tau} = \{G + iG'\}\bar{\gamma} \quad (i = \sqrt{-1}) \tag{14}$$

where $\bar{\tau}$ and $\bar{\gamma}$ are complex shear stress and complex shear strain, respectively, and G and G' are shear modulus and loss modulus, respectively. Damping ratio η, the definition of which is illustrated in Fig. 1, is related to G and G' as

$$\eta = \frac{1}{2\pi}\frac{\Delta W}{W} = \frac{G'}{2G} \tag{15}$$

G' is related to energy dissipated per cycle of cyclic loading within a unit ΔW as

$$G' = \frac{1}{\pi\gamma^2}\Delta W \tag{16}$$

where γ is a single amplitude shear strain. It is interesting to examine the characteristics of G' itself. From Eqs. (10) and (15),

$$\begin{aligned} G'/\{G\}_{\gamma=10^{-6}} &= 2G\cdot\eta/\{G\}_{\gamma=10^{-6}} \\ &= 2\eta_{\max}\cdot g(X)\cdot X \end{aligned} \tag{17}$$

where $X = G/\{G\}_{\gamma=10^{-6}}$. Measured values of $G'/\{G\}_{\gamma=10^{-6}}$ are shown in Fig. 18. It is seen in Fig. 18 that with increasing γ from 10^{-4} to 10^{-2} $G'/\{G\}_{\gamma=10^{-6}}$ increases proportionally to the $\log\gamma$ in the beginning, has its maximum value of at around $\gamma = 5\times10^{-4}$ to 10^{-3} and then decreases. It is also shown in Fig. 18 that the shear strain amplitude at which $G'/\{G\}_{\gamma=10^{-6}}$ has its maximum value increases with increasing confining pressure and that the maximum value of $G'/\{G\}_{\gamma=10^{-6}}$ is not affected by confining pressure. When $\eta_{\max}$ and $g(X)$ are independent of confining pressure, it can be derived from Eq. (17) that the maximum value of $G'/\{G\}_{\gamma=10^{-6}}$ is not affected by confining pressure. Therefore, it can be said that the results shown in Fig. 18 also support the concept

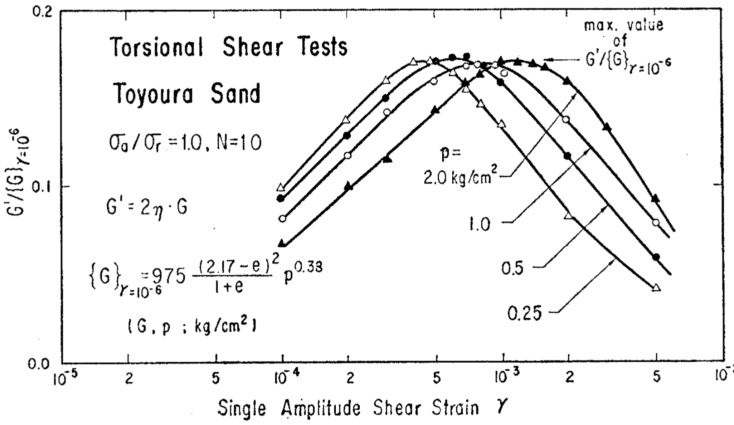

Fig. 18. $G'/\{G\}_{\gamma=10^{-6}}$ **versus** γ **relationship of Toyoura Sand**

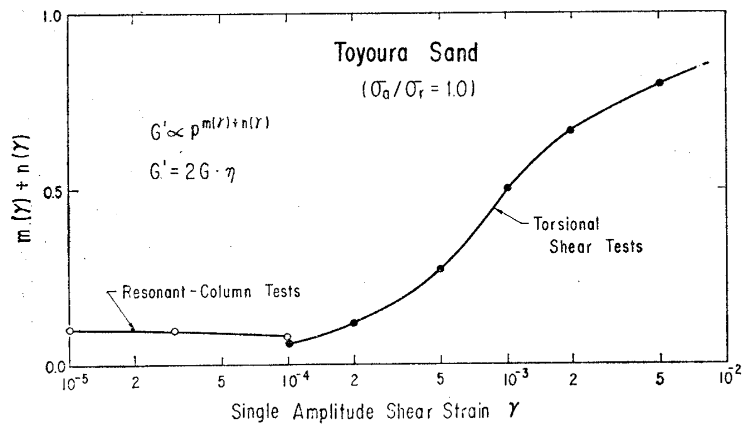

Fig. 19. $m(\gamma)+n(\gamma)$ **versus** γ **relationship of Toyoura Sand**

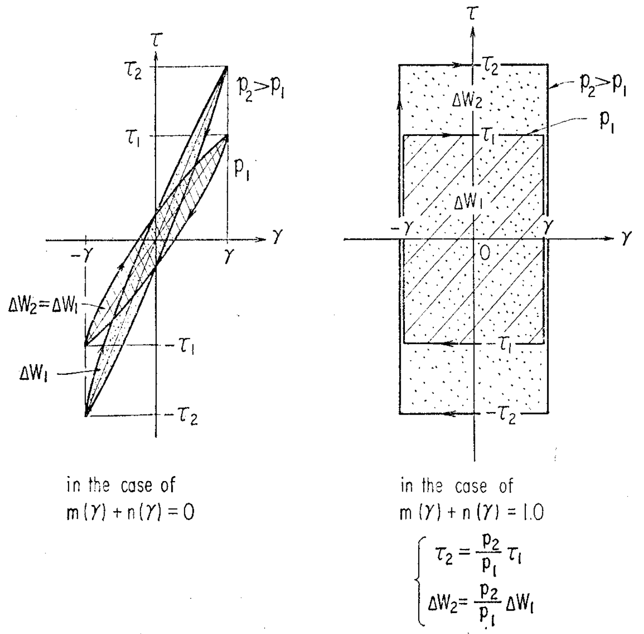

Fig. 20. Meanings of $m(\gamma)+n(\gamma)$

that η_{max} and $g(X)$ are independent of confining pressure.

As shear modulus G and damping ratio η are proportional to $p^{m(\gamma)}$ and $p^{n(\gamma)}$, respectively, $G'=2G\cdot\eta$ is expressed as

$$G'=L(\gamma)p^{m(\gamma)+n(\gamma)} \tag{18}$$

where $L(\gamma)$ is a function of shear strain. Furthermore, from Eqs. (16) and (18),

$$\Delta W=\pi\gamma^2 L(\gamma)p^{m(\gamma)+n(\gamma)} \tag{19}$$

The measured powers $m(\gamma)+n(\gamma)$ of Toyoura Sand are shown in Fig. 19. It is seen in Fig. 19 that with increasing shear strain amplitude from 10^{-6} to 10^{-2} the value of $m(\gamma)+n(\gamma)$ increases from a small value of about 0.1 at around $\gamma=10^{-6}$ to 10^{-4} to a large value of about 0.8 at $\gamma=5\times10^{-3}$. From this figure, it may be anticipated that $m(\gamma)+n(\gamma)$ will become unity when shear strain amplitude increases considerably larger than 10^{-2}. In viewing that $m(\gamma)+n(\gamma)$ is very small for shear strain amplitude of 10^{-4} or less, it seems that damping energy ΔW is almost not affected by confining pressure for a fixed value of γ as indicated by Eq. (19). The meaning of $m(\gamma)+n(\gamma)=0$ can be understood by Fig. 20. The value of $m(\gamma)+n(\gamma)$ of zero corresponds to the performance of a non-frictional material. On the other hand, the value of $m(\gamma)+n(\gamma)$ of unity corresponds to the state where damping energy ΔW is proportional to confining pressure. As illustrated in Fig. 20, this performance is that of a rigid-perfectly plastic material. At extremely large strains, granular materials behave as rigid-perfectly plastic materials. Therefore, in viewing that $m(\gamma)+n(\gamma)$ increases gradually from almost zero to unity with increasing shear strain amplitude, it is understood that with increasing shear strain amplitude behaviors of sands vary from those of non-frictional materials to those of rigid-perfectly plastic materials. These two extreme states, however, may not be attained in ordinary cases.

CONCLUSIONS

With use of a resonant-column apparatus and a torsional shear device, hysteretic damping ratios of reconstituted sands were obtained. Factors affecting damping ratios of sands were investigated. It was found from the test results of this investigation that (i) the effects of shear strain amplitude, confining pressure and number of cyclic loading on damping ratios of sands are significant, (ii) the effects of sand type are moderate and (iii) the effects of void ratio, moist conditions and methods of sample preparation are very small. On the basis of test results, empirical relationships between damping ratio η and shear modulus ratio $G/\{G\}_{\gamma=10^{-6}}$ or G/G_{max} were obtained. These relationships are not affected by void ratio, confining pressure and shear strain amplitude, and slightly affected by number of cyclic loading and sand type. When the values of $G/\{G\}_{\gamma=10^{-6}}$ are available, apporximate values of η for ordinary natural sands can be evaluated from $G/\{G\}_{\gamma=10^{-6}}$ using the solid curve shown in Fig. 17 which represents the average relationship between η and $G/\{G\}_{\gamma=10^{-6}}$ of non-clean natural sands tested in this investigation.

ACKNOWLEDGMENT

The authors wish to express their appreciations to Mr. Seiichi Yoshida of Ground Vibration Section, the Public Works Research Institute and Mr. Hideo Sudo and Mr. Shinji Fukushima, graduate students of Nihon University, for their helpful cooperations in conducting a number of experiments.

NOTATION

e = void ratio
$f(\gamma) = [G/\{G\}_{\gamma=10^{-6}}]_{p=1.0\text{kg/cm}^2}$
G = shear modulus
G' = loss modulus $= 2G\cdot\eta$
$\{G\}_{\gamma=10^{-6}}$ = shear modulus at $\gamma=10^{-6}$
G_{max} = shear modulus at $\gamma=0$ or $\gamma=\gamma_e$ (elastic strain)
$g(X)$ = a function of $X=G/\{G\}_{\gamma=10^{-6}}$
$m(\gamma)$ = power of mean principal stress p with respect to shear modulus
$m'(\gamma) = m(\gamma) - m(\gamma=10^{-6})$
$n(\gamma)$ = power of mean principal stress p with respect to damping ratio
N = number of cyclic loading
p = mean principal stress $= \frac{1}{3}(\sigma_a + 2\sigma_r)$
γ = single amplitude shear strain
τ = shear stress
η = hysteretic damping ratio $= \frac{1}{2\pi}\frac{\Delta W}{W}$
η_{max} = the maximum value of η for $G=0$
σ_a, σ_r = axial and radial stresses

REFERENCES

1) Drnevich, V. P. and Richart, F. E., Jr. (1970) : "Dynamic prestraining of dry sand," Journal of SMF Div., Proc., ASCE, Vol. 96, No. SM 2, pp. 453-469.
2) Hardin, B. O. (1965) : "The nature of damping in sands," Journal of SMF Div., Proc., ASCE, Vol. 91, No. SM 1, January, pp. 63-97.
3) Hardin, B. O. and Drnevich, V. P. (1972 a) : "Shear modulus and damping in soils I, Measurements and parameter effects," Journal of SMF Div., Proc., ASCE, Vol. 98, No. SM 6, pp. 603-624.
4) Hardin, B. O. and Drnevich, V. P. (1972 b) : "Shear modulus and damping in soils II, Design equations and curves," Journal of SMF DIV., Proc., ASCE, Vol. 98, No. SM 7, July, pp. 667-692.
5) Hara, A., Niwa, M. and Banno, T. (1973) : "Dynamic properties of saturated cohesive soils," Annual Report, Vol. 22, Kajima Institute of Construction Technology (in Japanese).
6) Iwasaki, T. and Tatsuoka, F. (1977) : "Effects of grain size and grading on dynamic shear moduli of sands," Soils and Foundations, Vol. 17, No. 3, pp. 19-35.

7) Iwasaki, T., Tatsuoka, F. and Y. Takagi, (1978) : "Shear moduli of sands under cyclic torsional shear loading," Soils and Foundations, Vol. 18, No. 1, pp. 39-56.
8) Kuribayashi, E., Iwasaki, T. and Tatsuoka, F. (1975) : "Effects of stress-strain conditions on dynamic properties of sands," Proc. of Japanese Society of Civil Engineers, No. 242, Oct., pp. 105-114.
9) Lazan, B. J. (1968) : Damping of Materials and Members in Structual Mechanics, Pergamon Press Ltd., London.
10) Seed, H. B. and Idriss, I. M. (1970) : "Shear moduli and damping factors for dynamic response analyses," Earthquake Eng. Res. Cen., Univ. of Cal. Berkeley, Cal., Rep. No. EERC 70-10.
11) Sherif, M. A. and Ishibashi, I. (1976) : "Dynamic shear moduli for dry sands," J. GTD, Proc., ASCE, Vol. 102, No. GT 11, pp. 1171-1184.
12) Sherif, M. A., Ishibashi, I. and Gaddah, A. H. (1977) : "Damping ratio for dry sands," J. GTD, Proc., ASCE, Vol. 103, No. GT 7, pp. 743-756.
13) Silver, M. L. and Seed, H. B. (1971) : "Deformation characteristics of sands under cyclic loading," Journal of SMF Div. Proc., ASCE, Vol. 97, No. SM 8, pp. 1081-1098.
14) Sugimoto, M., Susuki, Y., Terada, K. and Watanabe, T. (1974) : "Study on dynamic properties of soils (Part III)," Proc., 9 th Annual Meeting of Japanese Society of Soil Mech. Found. Eng., pp. 327-330 (in Japanese).
15) Yoshimi, Y. et al. (1976) : "Report of committee on dynamic properties of soils," Building Research Institute, Ministry of Construction.

(Received November 15, 1977)